Structure, exchange interactions, and magnetic phase transition of $Er_2Fe_{17-x}Al_x$ intermetallic compounds

Zhao-hua Cheng,* Bao-gen Shen, Qi-wei Yan, and Hui-qun Guo
State Key Laboratory of Magnetism, Institute of Physics & Center of Condensed Matter Physics, Chinese Academy of Sciences, Beijing 100080, People's Republic of China

Dong-feng Chen, Cheng Gou, and Kai Sun
China Institute of Atomic Energy, P.O. Box 275-30, Beijing 102413, People's Republic of China

F. R. de Boer and K. H. J. Buschow
Van der Waals–Zeeman Institute, University of Amsterdam, Valckenierstraat 65, 1018 XE Amsterdam, The Netherlands
(Received 18 June 1997; revised manuscript received 2 February 1998)

We present the effect of aluminum substitution on the structure, exchange interactions, and magnetic phase transitions of the intermetallic compound Er_2Fe_{17}. All samples have a hexagonal Th_2Ni_{17}-type structure or a rhombohedral Th_2Zn_{17}-type structure. The replacement of Fe by Al results in an approximately linear increase in the unit-cell volumes at a rate of 9.3 $Å^3$ per Al atom. The Al atoms preferentially occupy $12k$ $(18h)$ and $12j$ $(18f)$ sites at low Al concentration, while they prefer strongly to occupy $6c$ $(4f)$ and $18f$ $(12j)$ sites at high aluminum concentration. The Curie temperature is found to increase at first, form a maximum value at $x=3$, and then to decrease monotonically with increasing Al concentration. The exchange-coupling constant between $3d$ and $4f$ sublattices, J_{RT}, was obtained from fitting M-T curves for some of the samples. The intersublattice molecular-field coefficient n_{RT} and hence the R-T exchange-coupling constant J_{RT} have been also determined on the basis of magnetization curves at the compensation temperature. The exchange-coupling constant J_{RT} shows almost no obvious composition dependence, while the exchange-coupling constant J_{TT} is strongly dependent on the Al concentration. The composition dependence of the $3d$ sublattice exchange interaction is discussed in terms of bond lengths and atomic preferential occupancies. It is noteworthy that the substitution of Al has a significant effect on the magnetocrystalline anisotropies of both the Er sublattice and the Fe sublattice in $Er_2Fe_{17-x}Al_x$ compounds. The temperature and composition dependence of the easy magnetization direction suggests that the second-order crystal electric-field coefficient A_{20} changes its sign from negative to positive with increasing Al concentration up to $x>7$. [S0163-1829(98)02721-0]

I. INTRODUCTION

In the search for iron-rich new permanent magnet materials, the discovery of $R_2Fe_{17}(C, N, H)_x$ (R=rare-earth elements) obtained by the gas-solid reaction method has attracted considerable research activity.[1–3] $Sm_2Fe_{17}(C, N)_x$ is a very promising candidate as a permanent-magnet material. In order to overcome the drawback of its poor thermal stability, which restricts its practical application as a sintered magnet, Shen and co-workers[4,5] found that the substitution of Ga, Al, or Si for Fe in $Sm_2Fe_{17}C_x$ can stabilize the high-carbon rare-earth compounds with 2:17-type structure. The arc-melted carbides are found to retain the 2:17 structure even at temperature above 1200 °C. Shen and co-workers have prepared single-phase $R_2Fe_{17-x}Ga_xC_2$ compounds by arc melting and found that the Curie temperature increases initially and then decreases with Ga substitution while M_s decreases monotonically. These compounds have anisotropy fields exceeding 12 T.[4,5] Cheng and co-workers found a similar behavior in $Sm_2Fe_{17-x}Al_xC$, where the $x=2$ compound has an anisotropy field of 11 T.[6,7] The increase in Curie temperature with Al, Ga, and C has been attributed to the expansion of Fe-Fe bonds that compensates more for the dilution of the Fe sublattice. The high-temperature stability of the arc-melted carbides indicates that carbon is more strongly bonded than nitrogen in the samples formed by gas-solid reaction. These arc-melted carbides can be used as raw materials of high-performance sintered permanent magnets due to their high Curie temperature, strongly uniaxial anisotropy, as well as high-temperature stability.

Magnetocrystalline anisotropy and Curie temperature are the fundamental intrinsic magnetic parameters of permanent magnets and attract ever-growing attention from both experimentalists and theoreticians. Large values of the uniaxial magnetocrystalline anisotropy are required to achieve high coercivities, and high Curie temperature can guarantee the magnets to have low-temperature coefficients of the hard magnetic properties so that they can be applied over a wide temperature range. The facts that all R_2Fe_{17} binary compounds have low Curie temperatures and exhibit easy-plane anisotropy restrict their possible application as permanent magnets. Recently, it was found that the substitution of Ga, Al, or Si could not only facilitate the formation of R_2Fe_{17} carbides with high carbon concentration, but also increase significantly the Curie temperature. Furthermore, the easy magnetization direction (EMD) of $R_2Fe_{17-x}M_x$ (M=Ga or Al) alloys can be modified by the introduction of M atoms.[8–11] Low concentrations of Ga or Al substitution in

 © 1998 The American Physical Society

Sm_2Fe_{17} results in a change in EMD from basal plane to c axis without the presence of interstitial N or C atoms, while further substitution leads to a change from c axis to plane again. A reversal change in EMD has been found in $R_2Fe_{17-x}Ga_x$ with $R=$ Tb, Dy, Ho, Er, Tm. The Fe sublattice can also exhibit uniaxial anisotropy at room temperature when the Ga concentration is very high ($x \geqslant 7$). The change in EMD implies that the crystal electric field (CEF) coefficients at the R site are significantly influenced by the substituted atoms and this is worth more detailed investigation.

Knowing the intrinsic magnetic properties of the $R_2Fe_{17-x}M_x$ ($M=$ Ga or Al) series is the first step in understanding the basic magnetic properties of the interstitial compounds derived from them. From the application point of view, these series are not very promising. However, from a fundamental point of view, they provide a very good opportunity to investigate the exchange interactions and anisotropies of the $3d$ and $4f$ sublattices because Al or Ga atoms can substitute for Fe up to a very high concentration without changing the crystal structure, except for the unit-cell volume expansion. In this paper, the site occupancies of substituted atoms, exchange interactions between $3d$ and $4f$ sublattices, and the magnetocrystalline anisotropies of $3d$ and $4f$ sublattices in $Er_2Fe_{17-x}Al_x$ compounds have been investigated by means of magnetization and ac susceptibility measurements, x-ray diffraction (XRD), and neutron diffraction (ND). The reason for selecting $R=$ Er is twofold. First, in the case of the Er_2Fe_{17} compound, the Fe sublattice exhibits planar anisotropy, while the Er-sublattice anisotropy is expected to be uniaxial on the basis of the CEF effect in R_2Fe_{17} compounds. Therefore, spin reorientations may occur in $Er_2Fe_{17-x}Al_x$, either due to the temperature-induced competition between the Er and Fe sublattice anisotropies or due to the temperature-induced changes in the Er sublattice only. Second, the antiferromagnetic coupling between Er and Fe atoms allows us to investigate the intersublattice molecular-field coefficient n_{RT} by means of the magnetization curves of $Er_2Fe_{17-x}Al_x$ compounds at the compensation temperature. The temperature and composition dependence of magnetocrystalline anisotropy are explained in terms of a sign reversal of the second-order CEF coefficient A_{20} from negative to positive when the Al concentration increases up to $x>7$.

II. EXPERIMENTAL DETAILS

The samples of $Er_2Fe_{17-x}Al_x$ ($0 \leqslant x \leqslant 9$) were prepared by arc melting in an argon atmosphere of high purity. The elements used were at least 99.9% pure. An excess of 5% Er was added to compensate for the evaporation loss during melting. In order to ensure good homogeneity, the ingots were remelted at least four times, then annealed under an argon atmosphere at 1400 K for 5 days, followed by quenching into water. The ingots were ground to yield powders. The magnetic powders were oriented in an applied field of 1 T and fixed by means of epoxy resin to investigate the magnetocrystalline anisotropy.

The structural properties were investigated by means of XRD and ND. XRD experiments were performed on powder samples using Cu $K\alpha$ radiation to determine the crystal structure, lattice constants, and unit-cell volume. The powder ND experiments were employed to investigate the crystal structure, the occupancies of substituted atoms, as well as the magnetic structure.

The powder ND patterns of $Er_2Fe_{15}Al_2$ and $Er_2Fe_{12}Al_5$ were collected on a triple-axis spectrometer at China Institute of Atomic Energy at room temperature, while the pattern of $Y_2Fe_9Al_8$ was collected at 10 K to investigate the Fe sublattice anisotropy. The diffraction data were analyzed by Izumi's Rietveld structure refinement program RIETEN.[12]

The magnetization curves were measured by using an extracting sample magnetometer with a magnetic field ranging from 0 to 6.5 T. The saturation magnetization was obtained from fitting the experimental data of $M(B)$ vs B using the law of approach to saturation. The values of the Curie temperature were derived from the temperature dependence of magnetization $M(T)$ curves measured in a field of 0.05 T or ac susceptibility measured by an ac susceptibility magnetometer in a weak field of less than 0.0001 T at a frequency of 220 Hz.

III. RESULTS AND DISCUSSIONS

A. Structural properties

XRD patterns indicate that all samples are almost single phase with a hexagonal Th_2Ni_{17}-type structure or a rhombohedral Th_2Zn_{17}-type structure. The samples with low Al concentration crystallize in the hexagonal Th_2Ni_{17}-type structure, while those with high Al concentration crystallize in the rhombohedral Th_2Zn_{17}-type structure. The lattice constants a, c and the unit-cell volume v are summarized in Table I. In order to compare the volumes of the hexagonal cell with the rhombohedral one, we have multiplied the former by a factor of $\frac{3}{2}$. It can be found that the substitution of larger Al atoms for Fe atoms leads to an approximately linear increase in the unit-cell volumes at a rate of 9.3 $Å^3$ per Al atom.

The atomic occupancies were investigated by means of ND pattern on the powder samples of $Er_2Fe_{15}Al_2$ and $Er_2Fe_{12}Al_5$ at room temperature and $Y_2Fe_9Al_8$ at 10 K. For example, the ND patterns of $Er_2Fe_{15}Al_2$ and $Er_2Fe_{12}Al_5$ are shown in Fig. 1. The crystallographic parameters of the Th_2Ni_{17}- or Th_2Zn_{17}-type R-Fe compounds were used to start the refinement. The rhombohedral compound has only one crystallographically nonequivalent R site ($6c$), while the hexagonal compound has two crystallographically nonequivalent R sites ($2b$ and $2d$). These sites are, however, characterized by a quite similar local atomic arrangement of Fe atoms and a slightly different arrangement of the R atoms. The hexagonal $4f$, $6g$, $12j$, and $12k$ sites correspond to the rhombohedral $6c$, $9d$, $18f$, and $18h$ sites, respectively. Initially, it was assumed that the Al and Fe atoms occupy the four nonequivalent sites statistically. According to the chemical concentration and with the linear constraint condition, the sum of the fractional occupancies of Fe and Al atoms on each of these four sites was fixed to be equal to 1.0. The initial magnetic moments were taken equal to $2.0\mu_B$, $-1.0\mu_B$, and $0.0\mu_B$ for Fe, Er, and Y atoms, respectively, and all magnetic moments being in a parallel arrangement in a plane perpendicular to the sixfold axes. Refined values of the lattice and positional parameters, atomic occupancies, and magnetic moments of $Er_2Fe_{15}Al_2$ and $Er_2Fe_{12}Al_5$ at room

TABLE I. The structural and magnetic properties of $Er_2Fe_{17-x}Al_x$ compounds.

	a (Å)	c (Å)	v (Å^3)	M_s (μ_B/f.u.)	M_T (μ_B/f.u.)	μ_{Fe} (μ_B)	T_c (K)	T_{comp} (K)	J_{TT}/k_B (K)
$x=0$	8.455	8.270 (12.405)	510.78 (766.17)	16.9	34.9	2.05	297		23.7
$x=1$	8.477	8.303 (12.454)	516.71 (775.06)	13.6	31.6	1.98	363		35.4
$x=2$	8.511	8.319 (12.478)	521.87 (782.80)	10.6	28.6	1.91	396		45.6
$x=3$	8.535	8.339 (12.508)	526.08 (789.12)	7.4	25.4	1.81	407		56.2
$x=4$	8.590	12.532	800.82	5.2	23.2	1.78	391		61.5
$x=5$	8.618	12.576	808.88	3.3	21.3	1.77	338		59.5
$x=6$	8.667	12.603	819.86	0.7	18.7	1.70	249		51.5
$x=7$	8.710	12.622	829.27	−2.4	15.6	1.56	182	66.5	42.7
$x=8$	8.755	12.655	840.05	−3.7	14.3	1.59	146	84.0	37.5
$x=9$	8.782	12.731	850.32	−5.7	12.3	1.54	142	94.0	46.7

temperature and of $Y_2Fe_9Al_8$ at 10 K are summarized in Table II. The room-temperature magnetic moments of $Er_2Fe_{17-x}Al_x$ compounds stay in the basal plane $[h00]$ and the magnetic moments of all Fe atoms display ferromagnetic coupling, but the magnetic moments of Er and Fe are antiferromagnetically coupled. It is noteworthy that the Fe magnetic moments of $Y_2Fe_9Al_8$ are along [001] at low temperature. The magnetic moments orientation will be discussed in detail in the following section. The Rietveld structure analyses show an obvious concentration dependence fractional occupancy of Al on each of the four crystallographic sites, $6c(4f)$, $9d(6g)$, $18f(12j)$, and $18h(12k)$, in $R_2Fe_{17-x}Al_x$ (Fig. 2). For comparison, the results that would be expected for a random substitution of Al on the Fe sites are also presented in Fig. 2. It can be seen from Fig. 2 that the Al atoms prefer $18f(12j)$ and $18h(12k)$ sites at low Al concentration, whereas they prefer strongly to occupy $6c(4f)$ and $18f(12j)$ sites at high Al concentration. The $6c(4f)$ site initially does not take up aluminum, but at high Al content up to 80% of this site is occupied by Al atoms for $Y_2Fe_9Al_8$. The $9d(6g)$ site excludes Al at all concentrations. The Al fractional occupancies at the $18f(12j)$ site increase monotically, but those at the $18h(12k)$ site become saturated at about 40%. This result is very similar to that of $Nd_2Fe_{17-x}Al_x$.[13] The atomic preferential occupancies are determined to a large extent by the Wigner-Seitz cell volume.[13,14] Because Al atoms have larger metallic radii than iron, they prefer to occupy the $6c(4f)$ site which has, especially in higher aluminum concentration, the largest Wigner-Seitz cell volume, and avoid occupying the $9d(6g)$ site that has the smallest Wigner-Seitz cell volume. If a site is unoccupied by Al, its near neighbors prefer to accept Al atoms. Thus, because the $9d(6g)$ site has four $18f(12j)$ and four $18h(12k)$ sites as near neighbors, these latter sites are in favor of accepting Al atoms.

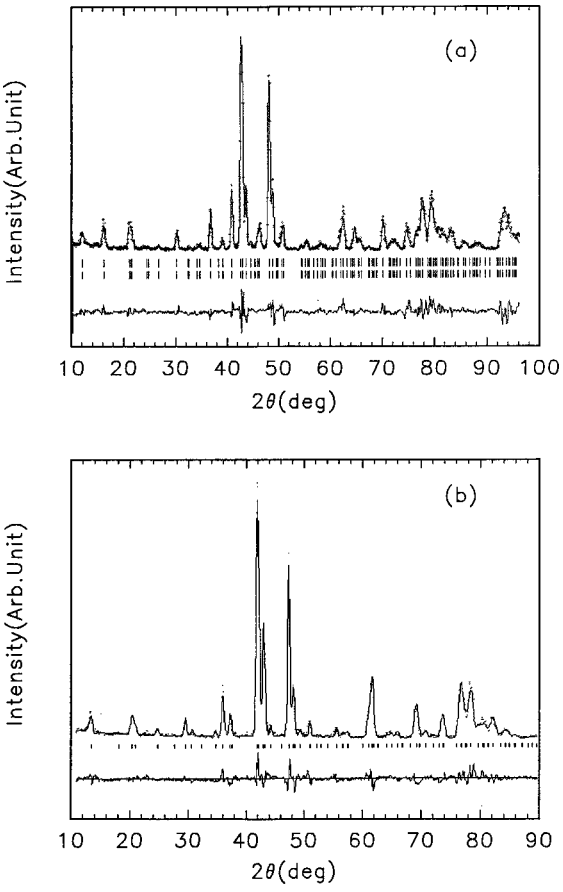

FIG. 1. Powder neutron-diffraction patterns of $Er_2Fe_{17-x}Al_x$ compounds with (a) $x=2$ and (b) $x=5$ at room temperature.

B. Saturation magnetization and magnetic moments

Figure 3 shows the magnetization curves of $Er_2Fe_{17-x}Al_x$ compounds measured at 1.5 K. It is found that the saturation magnetization decreases linearly with increasing Al concentration, and this decrease is much faster than in the case of a simple magnetic dilution as shown by the dotted line in Fig. 4. This implies that the decrease in saturation magnetization is not only due to the simple magnetic dilution, but also due to the decrease of Fe magnetic moments. The antiparallel coupling between the R spin moment and the Fe moment leads to ferrimagnetism for the heavy rare-earth compounds.

TABLE II. Crystallographic and magnetic parameters of $Er_2Fe_{15}Al_2$ and $Er_2Fe_{12}Al_5$ at room temperature and $Y_2Fe_9Al_8$ at 10 K.

Atom site	Occupancy	x	y	z	$M(\mu_B)$
$Er_2Fe_{15}Al_2$	P_{63}/mmc	$a=b=8.521(1)$ Å		$c=8.335(8)$ Å	$v=524.1$ Å^3
Er($2b$)	1.00	0.000	0.000	0.250	$-3.12(28)$[a]
Er($2d$)	1.00	0.333(3)	0.666(7)	0.750	$-3.09(28)$[a]
Fe($4f$)	1.00	0.333(3)	0.666(7)	0.104(1)	2.20(30)[a]
Fe($6g$)	1.00	0.500	0.000	0.000	0.66(33)[a]
Fe($12j$)	0.79	0.330(1)	$-0.041(1)$	0.250	0.88(28)[a]
Fe($12k$)	0.87	0.165(1)	0.330(1)	0.983(1)	1.56(28)[a]
Al($12j$)	0.21	0.330(1)	$-0.041(1)$	0.250	0.00
Al($12k$)	0.13	0.165(1)	0.330(1)	0.983(1)	0.00
$Er_2Fe_{12}Al_5$	$R\bar{3}m$	$a=b=8.645(2)$ Å		$c=12.648(3)$ Å	$v=818.60$ Å^3
Er($6c$)	1.00	0.000	0.000	0.340(2)	$-2.15(16)$[a]
Fe($6c$)	0.63	0.000	0.000	0.098(2)	0.30(2)[a]
Fe($9d$)	1.00	0.500	0.000	0.500	0.50(2)[a]
Fe($18f$)	0.65	0.295(1)	0.000	0.000	0.30(2)[a]
Fe($18h$)	0.64	0.502(1)	0.498(1)	0.157(1)	0.70(2)[a]
Al($6c$)	0.37	0.000	0.000	0.098(2)	0.00
Al($18f$)	0.35	0.295(1)	0.000	0.000	0.00
Al($18h$)	0.36	0.502(1)	0.498(1)	0.157(1)	0.00
$Y_2Fe_9Al_8$	$R\bar{3}m$	$a=b=8.7446(6)$ Å		$c=12.6728(1)$ Å	$v=839.23$ Å^3
Y($6c$)	1.00	0.000	0.000	0.347(5)	0.00
Fe($6c$)	0.20(1)	0.000	0.000	0.104(5)	1.60(2)[b]
Fe($9d$)	1.00	0.500	0.000	0.500	2.10(2)[b]
Fe($18f$)	0.29(1)	0.290(5)	0.000	0.000	1.80(2)[b]
Fe($18h$)	0.60(1)	0.501(5)	0.498(5)	0.158(5)	2.00(2)[b]
Al($6c$)	0.80(1)	0.000	0.000	0.107(5)	0.00
Al($18f$)	0.71(1)	0.290(5)	0.000	0.000	0.00
Al($18h$)	0.40	0.501(5)	0.498(5)	0.158(5)	0.00

[a]The magnetic moments are oriented along [h00] at room temperature.
[b]The magnetic moments are oriented along [001] at 10 K.

Accordingly, the saturation moments of $Er_2Fe_{17-x}Al_x$ compounds can be expressed by the equation

$$M_S = M_T - M_R = (17-x)\mu_{Fe} - 2\mu_{Er}, \quad (1)$$

where M_T is the magnetic moment of the T=(Fe, Al) sublattice and M_{Er} is the moment of the Er sublattice.

If we assume the Er magnetic moment is equal to the free-ion magnetic moment $\mu_{Er}=9.0\mu_B$, the average Fe mag-

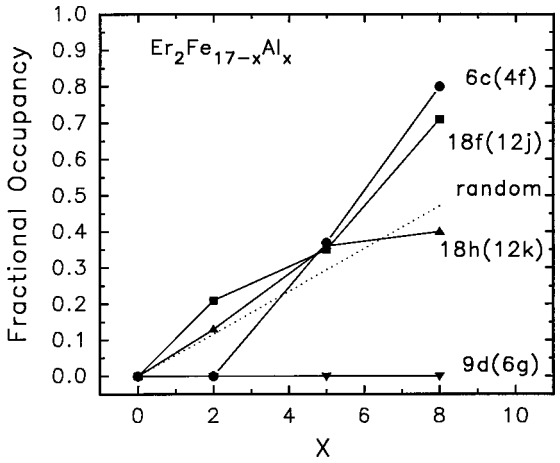

FIG. 2. Concentration dependence of the fractional occupancy on each of the four crystallographic sites [$6c(4f)$, $9d(6g)$, $18f(12j)$, and $18h(12k)$] in $R_2Fe_{17-x}Al_x$ (R=Er or Y). The dashed line represents the random substitution model.

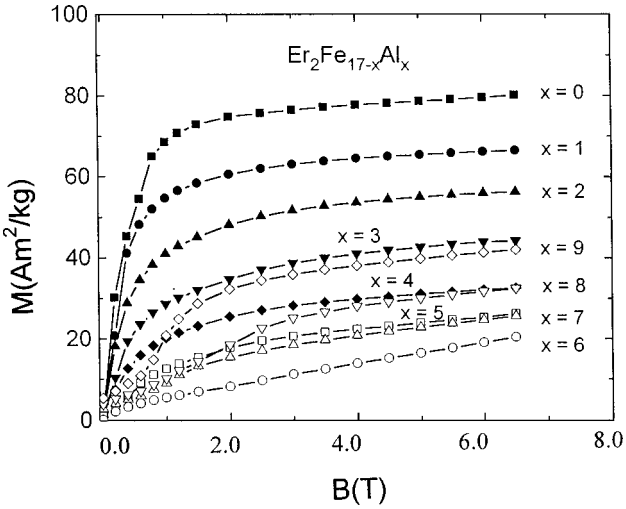

FIG. 3. Magnetization curves of $Er_2Fe_{17-x}Al_x$ compounds at 1.5 K.

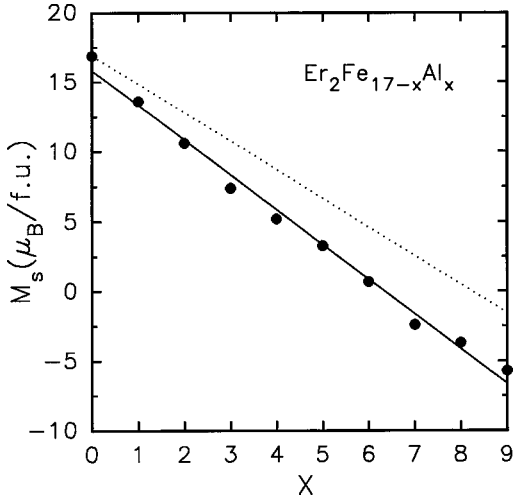

FIG. 4. Saturation magnetization of $Er_2Fe_{17-x}Al_x$ compounds at 1.5 K as a function of aluminum concentration. The dotted line represents the magnetization for simple magnetic dilution model.

netic moments μ_{Fe} of $Er_2Fe_{17-x}Al_x$ can be obtained. They are found to decrease with increasing Al concentration (Table I).

With increasing Al concentration, the T-sublattice moment will decrease. For the sample with $x \approx 6$, it is about equal to the Er sublattice moment at 1.5 K. The T-sublattice moments will be lower than the Er sublattice and therefore a negative value of the magnetic moment of $Er_2Fe_{17-x}Al_x$ is shown in Fig. 4 for $x > 6$.

C. Curie temperature, compensation temperature, and exchange interactions

Figure 5 illustrates the temperature dependence of the magnetization of $Er_2Fe_{17-x}Al_x$ compounds with $7 \leqslant x \leqslant 9$ measured by an extracting sample magnetometer in a magnetic field of 0.05 T. In order to avoid the effect of a strong magnetocrystalline anisotropy on the temperature dependence of the magnetization at low temperature, the samples

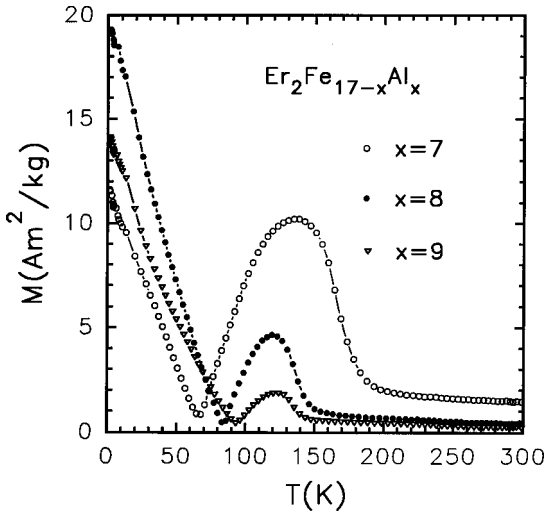

FIG. 5. Temperature dependence of the magnetization of $Er_2Fe_{17-x}Al_x$ compounds with $7 \leqslant x \leqslant 9$ in a magnetic field of 0.05 T.

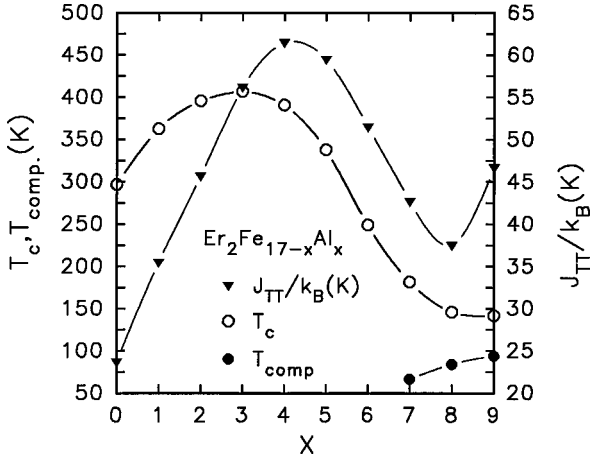

FIG. 6. Concentration dependence of Curie temperature T_C, compensation temperature T_{comp}, and the T-T exchange-coupling constant J_{TT}.

were cooled from room temperature to 1.5 K in a high magnetic field of 4 T, and then measured in a low magnetic field of 0.05 T. For these three samples, the T-sublattice magnetic moments are lower than those of the Er sublattice at 1.5 K. However, since the Er-sublattice moments decrease more rapidly than the T-sublattice moments with increasing temperature, they will become equal at a certain temperature. It can be seen that the compensation temperature T_{comp} is higher for higher Al concentration.

The concentration dependence of the Curie temperature T_c and the compensation temperature T_{comp} of $Er_2Fe_{17-x}Al_x$ are illustrated in Fig. 6. A small substitution of Al results in an enhancement of the Curie temperature from 297 K for $x=0$ to 407 K for $x=3$. Further substitution leads to a decrease in Curie temperature. The initial increase in Curie temperature is a common feature in $R_2Fe_{17-x}M_x$ (M=Ga or Al) intermetallic compounds.[8–11,15,16]

The Curie temperatures of R-T intermetallics are determined by the three different exchange-coupling constants: J_{TT}, J_{RT}, and J_{RR}. J_{TT} primarily governs the temperature dependence of the $3d$ moment and the Curie temperature T_c. The $3d$-$4f$ interaction J_{RT} has only a minor influence on the Curie temperature, especially for compounds rich in iron, such as R_2Fe_{17}, $R_2Fe_{14}B$, and $R(Fe,M)_{12}$. However, it dominates the molecular field experienced by the rare-earth moment that, in turn, determines the temperature dependence of the magnetic moment and the magnetocrystalline anisotropy of the rare-earth ions. The R-R interaction is generally neglected because it is smaller than the T-T and R-T interaction. In addition, there are few R-R bonds in the Fe-rich compounds. Thus, the standard molecular-field expression of the Curie temperature for two-sublattice R-T compounds can be written as[17]

$$3kT_C = a_{TT} + [a_{TT}^2 + 4a_{RT}a_{TR}]^{1/2}, \tag{2}$$

where $a_{TT} = Z_{TT}J_{TT}S_T(S_T+1)$ and

$$a_{RT}a_{TR} = Z_{RT}Z_{TR}S_T(S_T+1)(g_R-1)^2J_R(J_R+1)J_{RT}^2,$$

where S_T, J_R are the spin moment and total moment of T and R ions, respectively. g_R is the Landé g factor of the R ions. Z_{ij} ($i=R$, $j=T$, or $i=T$, $j=R$) is the number of j

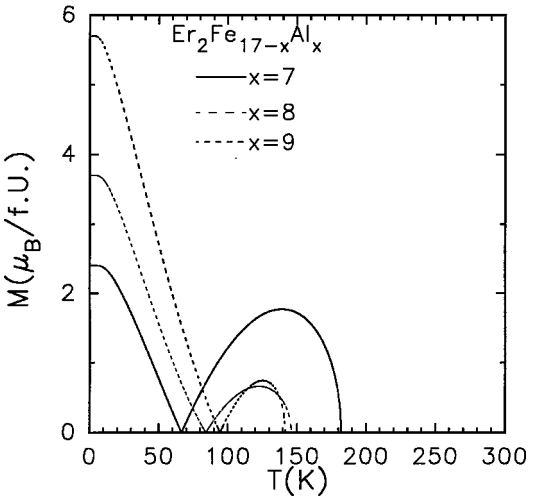

FIG. 7. Calculated spontaneous magnetization vs temperature curves of $Er_2Fe_{17-x}Al_x$ compounds with $7 \leqslant x \leqslant 9$ on the basis of the molecular-field model. In these calculations we used the following parameters: for $x=7$, $J_{ErT}=12.9$ K, $J_{TT}=42.7$ K, $J_T=0.459\mu_B$; for $x=8$, $J_{ErT}=11.6$ K, $J_{TT}=37.5$ K, $J_T=0.421\mu_B$; for $x=9$, $J_{ErT}=10.6$ K, $J_{TT}=46.7$ K, $J_T=0.362\mu_B$.

neighbors to an i atom. Z_{TT} is the number of T neighbors to a given T atom. The value of Z_{RT} is related to Z_{TR} via the relation $N_R Z_{RT}=N_T Z_{TR}$.[18] N_T and N_R are the numbers of T (Fe and Al) and R atoms per formula unit, respectively.

The exchange-coupling constant J_{TT} can be easily deduced from the Curie temperatures for compounds with $M_R=0$ ($a_{RT}a_{TR}=0$), such as $R=$ Y, La, and Lu. J_{RT} can be obtained either by high-field magnetization measurements on free powder particles of polycrystalline samples or by comparison of the difference in Curie temperatures between the compounds with $M_R \neq 0$ ($T_c=T_{c,R}$) and $M_R=0$ ($T_c=T_{c,0}$) such as $R=$ Y, La, Lu, using the high-temperature approximation of the molecular-field model:

$$J_{RT}^2=9k_B^2 T_{c,R}(T_{c,R}-T_{c,0})/4Z_{RT}Z_{TR}S_T(S_T+1) \times(g_R-1)^2 J_R(J_R+1). \quad (3)$$

In the first model, very high magnetic fields are required. Because the magnetic field available to many laboratories is limited, it is difficult to determine J_{RT} precisely in many cases. The second method is generally used under the assumption that J_{TT} is constant regardless of which R element is considered in $R_2Fe_{17-x}Al_x$. Problems in applying Eq. (3) may arise when the T-T interaction varies across the R series, since J_{TT} may depend strongly on the interatomic distance between the nearest-neighbor magnetic atoms. The lattice constants of R_2Fe_{17}, and consequently, the interatomic distance of Fe-Fe pairs, are not the same for different R elements considered here (Er and Y). Therefore, the assumption of the same value of J_{TT} among in these series is not realistic. In this work, we will determine J_{ErT} and J_{TT} on the basis of the molecular-field model by fitting the temperature dependence of the magnetization.

Figure 7 presents several M-T curves calculated for the $Er_2Fe_{17-x}Al_x$ compounds with $7 \leqslant x \leqslant 9$ by using the molecular-field expressions. In fitting the M-T curves, the external magnetic field is neglected since it is much lower than the molecular field. The values of $M_T(1.5\text{ K})$ (Table I) are used to replace those of $M_T(0)$ approximately. Only J_{RT} and J_{TT} are kept adjustable. Because our experimental data were obtained on polycrystalline powder samples in a low field, there is a considerable effect of the magnetocrystalline anisotropy on the magnetization. We therefore concentrated only on the experimental values of T_c and T_{comp} and the corresponding shapes of the $M(T)$ curves and do not expect the amplitudes of the calculated $M(T)$ curves in Fig. 7 to match those of the experimental curves in Fig. 5. The corresponding values of J_{ErT} are listed in Table III.

TABLE III. The intersublattice molecular-field coefficient n_{ErT}, the critical magnetic field $B_{crit,1}$ and $B_{crit,2}$, the molecular field at Er ions $b_{mol,Er}$.

	n_{ErT} (T f.u./μ_B)	$B_{mol,Er}$ (T)	$B_{crit,1}$ (T)	$B_{crit,2}$ (T)	J_{ErT}/k_B (K)[a]	J_{ErT}/k_B (K)[b]
$x=7$	2.34	36.5	5.6	78.6	8.44	12.9
$x=8$	2.34	33.5	8.7	75.6	8.44	11.6
$x=9$	2.37	29.2	13.5	71.8	8.55	10.6

[a]Exchange-coupling constant obtained from the magnetization curves at the compensation temperature.
[b]Exchange-coupling constant obtained from fitting the M-T curves.

For ferrimagnetic R-T powder particles that were free to orient themselves in the applied field, the field dependence of the magnetization can be described in fields below as[17,19–21]

$$B_{1,crit}=n_{RT}|M_R-M_T|, \quad (4)$$

M_R is perfectly antiparallel to M_T with $M=|M_R-M_T|$, and in fields above as

$$B_{2,crit}=n_{RT}|M_R+M_T|. \quad (5)$$

M_R is exactly parallel to M_T with $M=|M_R+M_T|$. In the intermediate field range $B_{1,crit}<B<B_{2,crit}$ the resultant magnetic moment is

$$M=B/n_{RT}. \quad (6)$$

At the compensation temperature $M_R(T_{comp})=M_T(T_{comp})$ the linear range with $M=B/n_{RT}$ starts at $B=0$ T. Experimentally, the field dependence of the magnetization close to the compensation temperature was found to be linear at all but the lowest field strengths (Fig. 8). From the slope of the linear parts, we have determined the values of the intersublattice molecular-field coefficient n_{ErT} at the compensation temperature. The Er-T exchange-coupling constant J_{ErT} can be directly obtained from the relation between J_{RT} and n_{RT}. The results are tabulated in Table III where it can be seen that the values of J_{ErT} obtained by the two methods described above are of comparable magnitude.

The values of J_{ErT} show no obvious dependence on the Al concentration in $Er_2Fe_{17-x}Al_x$ compounds. This result is in good agreement with previous work.[16] If we use the average value $J_{ErT}/k_B=10.1$ K, the T-T exchange-coupling constant J_{TT} can be obtained from Eq. (2). The values of J_{TT} are listed in Table I and as a function of Al concentration are plotted in Fig. 6. It can be seen that the effect of R-T ex-

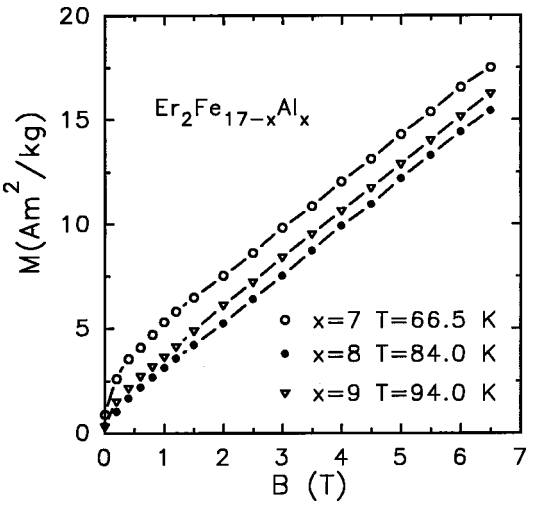

FIG. 8. Field dependence of the magnetization of $Er_2Fe_{17-x}Al_x$ compounds with $7 \leqslant x \leqslant 9$ close to the compensation temperatures.

change interaction on Curie temperature of $Er_2Fe_{17-x}Al_x$ compounds cannot be neglected.

Due to the short $6c$-$6c$ bond length, the $6c$ site is generally believed to be responsible for the low Curie temperature of the R_2Fe_{17} compounds. However, the ND results clearly indicate that the initial Curie temperature enhancement in $R_2Fe_{17-x}Al_x$ compounds is not a result of the removal of iron $6c$ ''dumbbell'' atoms by substitution of Al onto these sites, but that it has to be attributed to the overall increase in Fe-Fe bond lengths, which overcompensates the dilution of Fe atoms, although magnetic dilution becomes more important in determining the Curie temperature upon further substitution of the nonmagnetic Al atoms. It is noteworthy that the value of J_{TT} increases again at the highest Al concentrations. This phenomenon was also observed in other $R_2Fe_{17-x}Ga_x$ (R=Dy, Ho, Er, or Tm) compounds.[22–24] Simultaneously, the ND results demonstrate that the Al atoms strongly prefer to occupy the $6c$ site. The increase in T-T exchange interaction is perhaps related to the preferential substitution of Al for Fe onto this site. An investigation of the mechanism of this enhancement in J_{TT}, and hence, in Curie temperature is in progress.

D. Magnetocrystalline anisotropy and magnetic phase transition

In general, the overall magnetocrystalline anisotropy of R-T intermetallics is the sum of $4f$-sublattice and $3d$-sublattice anisotropies. In the case of R_2Fe_{17} compounds

$$K_{1,\mathrm{tot}} = 2K_{1,R} + K_{1,\mathrm{Fe}}, \tag{7}$$

where $K_{1,R}$ is the contribution of one R^{3+} ion to the anisotropy constant and $K_{1,\mathrm{Fe}}$ is the anisotropy constant of the Fe sublattice. In the first approximation, $K_{1,R}$ can be described as

$$K_{1,R} = -\tfrac{3}{2}\alpha_J A_{20}\langle r_{4f}^2\rangle\langle 3J_{R,z}^2 - J_R(J_R+1)\rangle, \tag{8}$$

where α_J is the second-order Stevens factor and A_{20} is the second-order CEF coefficient.

In the case of Er_2Fe_{17}, the Fe sublattice exhibits an easy-plane anisotropy, i.e., $K_{1,\mathrm{Fe}} < 0$, while the Er-sublattice anisotropy is dependent on the product of α_J and A_{20}. For the Er^{3+} ion, $\alpha_J > 0$. Hence, a negative A_{20} will make the Er-sublattice moments favor c-axis orientation at low temperature, $K_{1,\mathrm{Er}} > 0$. Although there are two crystallographically distinct sites in Er_2Fe_{17}, it was proved that the CEF anisotropy can be described using a single set of crystal-field parameters averaged over the two sites.[25–27] Values of $+17.9Ka_0^{-2}$ and $-8.9Ka_0^{-4}$ for the second- and the fourth-order CEF coefficients A_{20} and A_{40} respectively, have been deduced by Andreev *et al.* from magnetization studies up to 6 T.[25] According to these results, Er_2Fe_{17} compound would not follow the systematic of the Stevens factor α_J for the easy magnetization direction. In order to determine the CEF coefficients precisely, Garcia-Landa *et al.* investigated R_2Fe_{17} single crystals (R=Y, Dy, Ho, and Er) by means of high-field magnetization in a magnetic field up to 51 T, and obtained the values of $-24.58Ka_0^{-2}$ and $-11.88Ka_0^{-4}$ for A_{20} and A_{40}, respectively.[26] The value of the CEF coefficient A_{20} is in agreement with the results of the Mössbauer effect in Er_2Fe_{17}, for which the average value $A_{20} \approx -50 \pm 100Ka_0^{-2}$ was found.[28] If we only take into account the second-order CEF term, a value of $K_{1,R} = +7.0$ K/f.u. can be derived on the basis of Eq. (8), which is comparable with the value of $K_{1,\mathrm{Er}} = 8.5$ K/f.u. obtained by Franse *et al.*[29] Since its absolute value is much smaller and decreases more rapidly with increasing temperature than that of $K_{1,\mathrm{Fe}} = -50.4$ K/f.u. (at 4.2 K), no spin reorientation is expected to occur when the temperature varies between cryogenic temperatures and the Curie temperature.

The value of the ac susceptibility χ' of an intermetallic compound depends strongly on its magnetic anisotropy and domain-wall energy. It is proportional to $M_s^2/\sqrt{AK_1}$ for domain-wall displacement or M_s^2/K_1 for domain rotation. Both saturation magnetization M_s and anisotropy constant K_1 strongly vary with temperature; thus the shape of the χ' vs T curve is strongly affected by the temperature dependence of M_s and K_1. At the spin-reorientation temperature, the change of M_s is relatively smooth, while K_1 changes drastically, which is reflected as a kink in the χ' vs T curves. The spin-reorientation temperatures T_{sr} can be taken as the temperatures at which the first deviative of the ac susceptibility $d\chi'/dT$ reaches an extreme value (maximum or minimum). Measurements of temperature dependence of the ac susceptibility can be therefore used to detect temperature-induced magnetic-phase transitions. Figure 9 shows the temperature dependence of the χ' of $Er_2Fe_{17-x}Al_x$ compounds with x=1, 2, 3, and 4. An anomaly is visible for each of samples. The anomalies in χ' become more clear if $d\chi'/dT$ is plotted as a function of temperature, as shown in Fig. 10. Anomalies are also observed in the M-T curves measured a low magnetic field of 0.05 T (Fig. 11). Considering the temperature-induced competition between the planar Fe-sublattice anisotropy and the uniaxial Er-sublattice anisotropy, one can attribute these anomalies to spin reorientations. The spin-reorientation temperatures are found to increase first, have a maximum value at x=3, and then decrease. Similar results have also been observed in $Er_2Fe_{17-x}Ga_xC_2$ and $Er_2Fe_{17-x}Si_x$.[30,31] For the samples with x=5, 6, and 7,

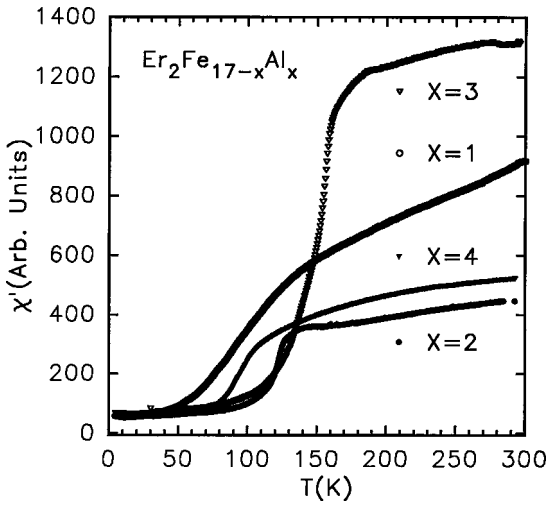

FIG. 9. Temperature dependence of the real component (χ') of the ac susceptibility of $Er_2Fe_{17-x}Al_x$ compounds with $x=1$, 2, 3, and 4.

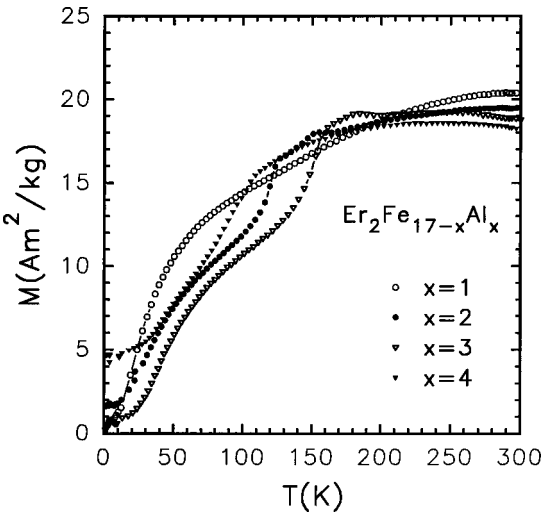

FIG. 11. Temperature dependence of the magnetization of $Er_2Fe_{17-x}Al_x$ compounds with $x=1$, 2, 3, and 4.

no spin reorientation was detected from the temperature dependence of the ac susceptibility. The sharp peaks at the temperatures of 246 and 182 K for the samples with $x=6$ and 7, respectively, correspond to their Curie temperatures (Fig. 12). These results suggest that the substitution of Al atoms has an effect not only on the Fe-sublattice anisotropy, but also on the Er-sublattice anisotropy.

In order to determine the contributions of these two sublattices to the overall anisotropy separately, one can choose the R elements without contribution to the R-sublattice anisotropy in $R_2Fe_{17-x}Al_x$. Thus, at first we studied the Fe-sublattice anisotropy by selecting $R=$ Y or Gd. The planar anisotropy constants $K_{1,Fe}$ of $Y_2Fe_{17-x}Al_x$ compounds with $x\leqslant 6$ have been obtained from the magnetization measurements on the magnetically aligned powders on the basis of a simple theoretical model proposed by Li *et al.*[32] They are weakened by Al substitution (Fig. 13). The nonlinear decrease of $K_{1,Fe}$ in absolute value implies that the fractional occupancies of Al atoms at the four nonequivalent sites are not the same and that the contributions of these four sites to the overall anisotropy are different.

Since the composition dependence of the Al and Ga atomic occupancies in $R_2Fe_{17-x}M_x$ ($M=$ Ga or Al) compounds is almost the same,[13,15,33,34] one can expect on the basis of the results obtained for $R_2Fe_{17-x}Ga_x$ that the further introduction of Al atoms results in an easy c-axis anisotropy of the Fe sublattice. Because $Y_2Fe_{10}Al_7$ cannot be magnetically aligned at room temperature due to its low Curie temperature, we aligned $Gd_2Fe_{10}Al_7$ powders instead of $Y_2Fe_{10}Al_7$ to investigate the Fe-sublattice anisotropy. Easy c-axis anisotropy of the Fe sublattice was, however, not observed for $x\leqslant 7$, while for further increase in Al concentration the Curie temperature was lower than room temperature. Because of its capability of investigating microscopically the crystal and magnetic structure, ND study on $Y_2Fe_9Al_8$ has been undertaken at low temperature to determine the magnetic moment orientation. The refinement results, as summarized in Table II, indicate that the Fe moments are oriented

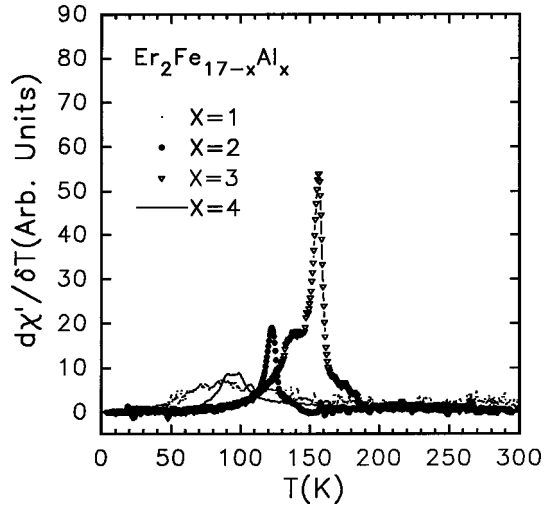

FIG. 10. Temperature dependence of the first derivative of ac susceptibility $d\chi'/dT$ of $Er_2Fe_{17-x}Al_x$ compounds with $x=1$, 2, 3, and 4.

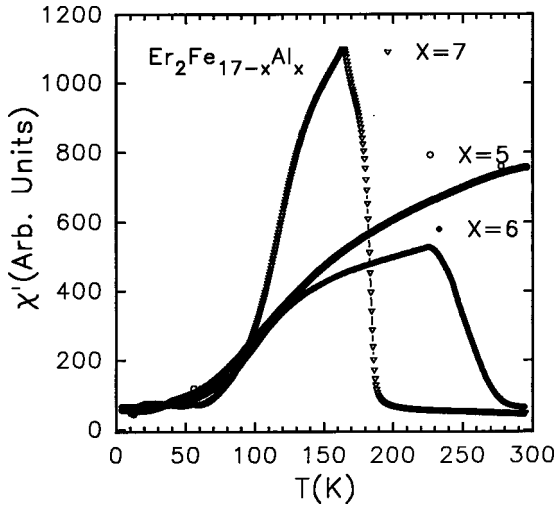

FIG. 12. Temperature dependence of the real component (χ') of the ac susceptibility of $Er_2Fe_{17-x}Al_x$ compounds with $x=5$, 6, and 7.

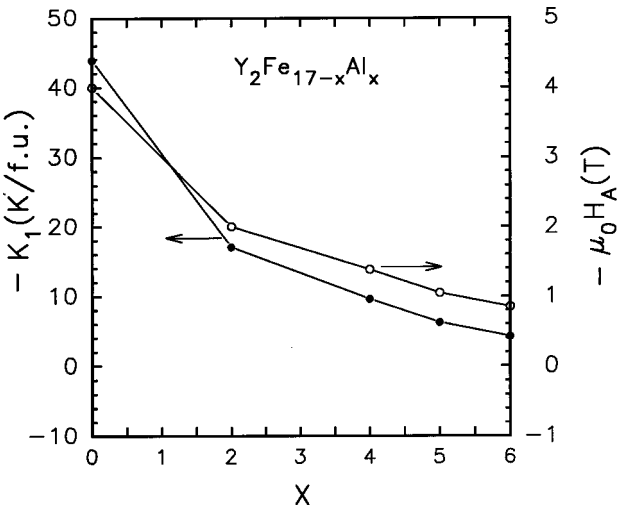

FIG. 13. Concentration dependence of the anisotropy constant K_I and the anisotropy fields $\mu_0 H_A$ of $Y_2Fe_{17-x}Al_x$ compounds.

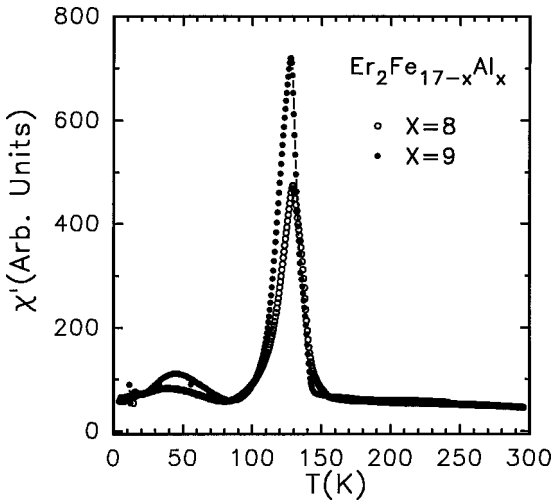

FIG. 14. Temperature dependence of the ac susceptibility of $Er_2Fe_{17-x}Al_x$ with $x=8$ and 9.

along [001]. This means that a uniaxial anisotropy of the Fe sublattice can be induced also by the introduction of Al atoms. Comparing the occupancies of Al atoms with those of Ga atoms,[13,15,33,34] one can deduce that the Al or Ga atoms preferentially occupy $6c$ and $18f$ sites, which may make a predominant contribution to the easy-plane anisotropy. When the Fe atoms at these sites are replaced by nonmagnetic atoms, a positive $K_{1,\mathrm{Fe}}$ may be obtained, that is, a uniaxial anisotropy of the Fe sublattice can be induced. A detailed investigation of the contribution of the individual sites to the overall anisotropy will be undertaken in the near future.

As can be seen in Fig. 13, the absolute value of the anisotropy constant $K_{1,\mathrm{Fe}}$ decreases from 50.4 K/f.u. for Y_2Fe_{17} to 17.0 K/f.u. for $Y_2Fe_{15}Al_2$ at 4.2 K. In view of the fact that for the sample $Er_2Fe_{15}Al_2$, the easy magnetization direction changes from basal plane to c axis with decreasing temperature, this suggests $K_{1,\mathrm{Er}}>17.0$ K/f.u. at 4.2 K. On the basis of Eq. (8), the value of A_{20} has been found to increase in negative value from $-24.58Ka_0^{-2}$ for Er_2Fe_{17} to more than $-29.85Ka_0^{-2}$ for $Er_2Fe_{14}Al_2$.

With decreasing temperature, no spin reorientation is found in the $Er_2Fe_{17-x}Al_x$ samples with $x=5$, 6, and 7. This implies that there are two possibilities: (1) $K_{1,\mathrm{Er}}>|K_{1,\mathrm{Fe}}|$ or (2) $K_{1,\mathrm{Er}}<|K_{1,\mathrm{Fe}}|$ at all temperatures. The first possibility can be excluded on the basis of ND results that $Er_2Fe_{12}Al_5$ exhibits easy-plane anisotropy at room temperature. Thus, it is only possible that $K_{1,\mathrm{Er}}<|K_{1,\mathrm{Fe}}|$ for the compounds with $x=5$, 6, and 7 at all temperatures. Thus, the value of $K_{1,\mathrm{Er}}$ also decreases with further increasing Al concentration. The easy c-axis anisotropy of the Er sublattice is not strong enough to overcome the planar anisotropy of the Fe sublattice. The decrease of $K_{1,\mathrm{Er}}$ is attributed to the A_{20} decreases in negative value with increasing Al concentration. For example, for the compound with $x=6$, $K_{1,\mathrm{Fe}}=-4.2$ K/f.u. at 4.2 K. This means that $K_{1,\mathrm{Er}}<4.2$ K/f.u. at 4.2 K. On the basis of Eq. (8), the absolute value of A_{20} will reduce to less than $14.75Ka_0^{-2}$ for $Er_2Fe_{10}Al_6$.

The temperature dependence of the ac susceptibility shows a sharp peak at 146 and 142 K and an anomaly at the temperature 38 and 44 K for the compounds with $x=8$ and 9, respectively (Fig. 14). The sharp peaks are attributed to the Curie temperatures, as are shown in Fig. 5, while the anomalies at low temperatures are related to spin reorientations. For the compounds with $x=8$ and 9, the uniaxial Fe-sublattice anisotropy dominates the overall magnetocrystalline anisotropy at high temperatures. Because the Er sublattice plays a more important role in determining the EMD at low temperature, it is reasonable to assume that the EMD changes from c axis to basal plane with decreasing temperature in these two compounds. The magnetic phase diagram of $Er_2Fe_{17-x}Al_x$ compounds is illustrated in Fig. 15. The fact that the EMD changes from c axis at high temperature to basal plane at low temperature implies that the sign of the second-order CEF coefficient A_{20} has changed from negative to positive with increasing Al substitution for $x \geqslant 8$. A similar effect of Ga substitution on the CEF coefficient was also observed in $Tb_2Fe_{17-x}Ga_x$ compounds by neutron-diffraction studies.[15]

Band-structure calculations have demonstrated that the second-order CEF coefficient A_{20} is determined predomi-

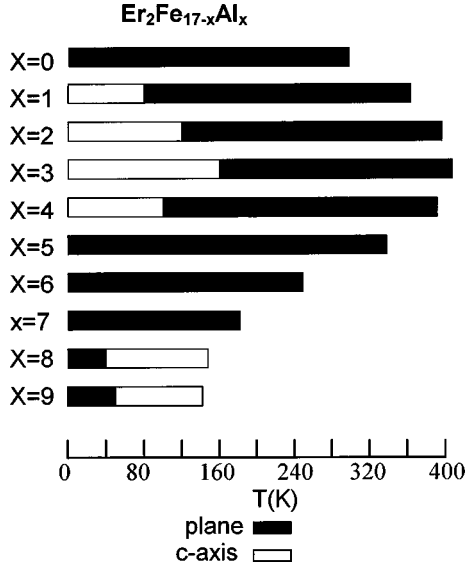

FIG. 15. Magnetic-phase diagram of $Er_2Fe_{17-x}Al_x$ compounds.

nantly by the R ions' $5d$ and $6p$ valence-electron charge asphericity.[35] It is strongly influenced by the variation of x in $R_2Fe_{17-x}Al_x$ because of the changing hybridization of the R ions' $5d$ and $6p$ valence-electron states with the valence-electron states of the neighbor atoms. Quite substantial changes in the magnitude and sign of the R valence-electron asphericity can be expected when Al preferentially substitutes into the nearest-neighbor sites of the R atoms.

IV. CONCLUSION

On the basis of the correlation between the Al atom occupancies in $Er_2Fe_{17-x}Al_x$ compounds and the Er- and T-sublattice anisotropies, it is reasonable to conclude the following. (1) The Fe atoms at $6c(4f)$ and $18f(12j)$ sites have a predominantly negative contribution to the anisotropy of Fe sublattice. When they are replaced by nonmagnetic Al atoms, a positive $K_{1,Fe}$, and hence, uniaxial anisotropy of the Fe sublattice may be obtained. (2) The preferential occupancies of the substituted atoms have a significant effect on the CEF coefficients at the Er site, and consequently, on the Er-sublattice anisotropy. The preferential occupancy of Al atoms of the $18h$ site, which is the nearest-neighbor of the Er site in the c-axis direction (different layer) seems to make the A_{20} values more negative, and hence to increase the uniaxial anisotropy of Er sublattice. Thus, a small degree of Al substitution can increase the spin-reorientation temperature of $Er_2Fe_{17-x}Al_x$ compounds. The preferential occupancies of Al atoms into the $18f$ site, which shares with the Er site at the same basal plane, appears to make the A_{20} values less negative, and finally lead to a sign reversal from negative to positive. Therefore, relatively high Al substitution in $Er_2Fe_{17-x}Al_x$ will change the EMD of the Er-sublattice moments from c axis to basal plane.

ACKNOWLEDGMENTS

This work was supported by the National Natural Sciences Foundation of China. The ac susceptibility was measured at the University of Amsterdam within the scientific exchange program between China and The Netherlands. Z.H.C. would like to thank the Alexander von Humboldt Foundation for financial support.

*Author to whom correspondence should be addressed. Present address: Max-Planck-Institut für Metallforschung, Heisenbergstrasse 1, D-70569 Stuttgart, Germany. FAX: 0049-711-6891010. Electronic address: cheng@vaxph.mpi-stuttgart.mpg.de

[1] J. M. D. Coey and H. Sun, J. Magn. Magn. Mater. **87**, L251 (1990).
[2] X. P. Zhong, R. J. Radwanski, F. R. de Boer, T. H. Jacobs, and K. H. J. Buschow, J. Magn. Magn. Mater. **86**, 333 (1990).
[3] X. Z. Wang, K. Donnely, J. M. D. Coey, B. Chevalier, J. Etourneau, and T. Berlureau, J. Mater. Sci. **23**, 329 (1988).
[4] B. G. Shen, L. S. Kong, F. W. Wang, and L. Cao, Appl. Phys. Lett. **63**, 2288 (1993).
[5] B. G. Shen, F. W. Wang, L. S. Kong, L. Cao, and H. Q. Guo, J. Magn. Magn. Mater. **127**, L267 (1993).
[6] Z. H. Cheng, B. G. Shen, F. W. Wang, J. X. Zhang, H. Y. Gong, and J. G. Zhao, J. Phys.: Condens. Matter **6**, L185 (1994).
[7] Z. H. Cheng, B. G. Shen, J. X. Zhang, F. W. Wang, H. Y. Gong, W. S. Zhan, and J. G. Zhao, J. Appl. Phys. **76**, 6734 (1994).
[8] B. G. Shen, F. W. Wang, L. S. Kong, and L. Cao, J. Phys.: Condens. Matter **5**, L685 (1993).
[9] Z. Wang and R. A. Dunlap, J. Phys.: Condens. Matter **5**, 2407 (1993).
[10] B. G. Shen, Z. H. Cheng, B. Liang, J. X. Zhang, H. Y. Gong, F. W. Wang, Q. W. Yan, and W. S. Zhan, Appl. Phys. Lett. **67**, 1621 (1995).
[11] Z. H. Cheng, B. G. Shen, B. Liang, J. X. Zhang, F. W. Wang, S. Y. Zhang, and H. Y. Gong, J. Phys.: Condens. Matter **7**, 4707 (1995).
[12] F. Izumi, Adv. X-ray Chem. Anal. Jpn. **14**, 43 (1977).
[13] W. B. Yelon, H. Xie, Gary J. Long, O. A. Pringle, F. Grandjean, and K. H. J. Buschow, J. Appl. Phys. **73**, 6029 (1993).
[14] L. Gelato, J. Appl. Crystallogr. **14**, 151 (1981).
[15] Z. Hu, W. B. Yelon, S. Mishra, Gary J. Long, O. A. Pringle, D. P. Middleton, K. H. J. Buschow, and F. Grandjean, J. Appl. Phys. **76**, 443 (1994).
[16] T. H. Jacobs, K. H. J. Buschow, G. F. Zhou, X. Li, and F. R. de Boer, J. Magn. Magn. Mater. **116**, 220 (1992).
[17] K. H. J. Buschow, Rep. Prog. Phys. **54**, 1123 (1991).
[18] P. E. Brommer, Physica B **173**, 277 (1991).
[19] R. Verhoef, R. J. Radwanski, and J. J. M. Franse, J. Magn. Magn. Mater. **89**, 176 (1991).
[20] X. C. Kou, R. Grössinger, G. Wiesinger, J. P. Liu, F. R. de Boer, I. Kleinschroth, and H. Kronmüller, Phys. Rev. B **51**, 8254 (1995).
[21] J. J. M. Franse and R. J. Radwanski, in *Handbook of Magnetic Materials*, edited by K. H. J. Buschow (North-Holland, Amsterdam, 1993), Vol. 7, p. 307; in *Rare-Earth Permanent Magnets*, edited by J. M. D. Coey (Clarendon, Oxford, 1996), p. 58.
[22] B. G. Shen, Z. H. Cheng, H. Y. Gong, B. Liang, Q. W. Yan, and W. S. Zhan, Solid State Commun. **95**, 813 (1995).
[23] B. G. Shen, Z. H. Cheng, B. Liang, H. Y. Gong, F. W. Wang, H. Tang, L. Cao, F. R. de Boer, and K. H. J. Buschow, J. Appl. Phys. **81**, 5173 (1997).
[24] Z. H. Cheng, Ph.D. thesis, Institute of Physics, Chinese Academy of Sciences, Beijing, 1995.
[25] A. V. Andreev, A. V. Dergayin, S. M. Zadvrokin, N. V. Kudrevatykh, V. N. Moskalev, R. Z. Levitin, Y. F. Popov, and R. Y. Yumaguchin, in *Physics of Magnetic Materials*, edited by D. D. Nishin (Sverdlovsk State University, Russia, 1985), pp. 21–49 (in Russian).
[26] B. Garcia-Landa, P. Q. Algarabel, M. R. Ibarra, F. E. Kayzel, and J. J. M. Franse, Phys. Rev. B **55**, 8313 (1997).
[27] K. Clausen and B. Lebech, J. Phys. C **50**, 95 (1982).
[28] P. C. M. Gubbens, A. A. Moolenaar, G. J. Boender, A. M. van der Kraan, T. H. Jacobs, and K. H. J. Buschow, J. Magn. Magn. Mater. **97**, 69 (1991).
[29] J. J. M. Franse, F. E. Kayzel, C. Marquina, R. J. Radwanski, and R. Verhoef, J. Alloys Compd. **181**, 95 (1992).
[30] B. G. Shen, H. Y. Gong, Z. H. Cheng, F. W. Wang, B. Liang, L. S. Kong, H. Q. Guo, W. S. Zhan, and J. G. Zhao, J. Magn. Magn. Mater. **151**, 111 (1995).
[31] B. Liang, B. G. Shen, Z. H. Cheng, H. Y. Gong, S. Y. Zhang, and J. X. Zhang, J. Phys.: Condens. Matter **7**, 4251 (1995).
[32] H. S. Li, R. C. Mohanty, A. Raman, C. G. Grenier, and R. E.

Ferrell, J. Magn. Magn. Mater. **166**, 365 (1997).
[33] Q. W. Yan, P. L. Zhang, X. D. Sun, B. G. Shen, Z. H. Cheng, C. Gou, D. F. Chen, R. Ridawan, H. Mujamilah, M. Gunawan, and P. Marsongkohadi, J. Phys.: Condens. Matter **8**, 1485 (1996).
[34] C. Gou, D. F. Chen, Q. W. Yan, P. L. Zhang, B. G. Shen, and Z. H. Cheng, J. Phys.: Condens. Matter **7**, 837 (1995).
[35] R. Coehoorn and K. H. J. Buschow, J. Appl. Phys. **69**, 5590 (1991).